© 2016. Published by The Company of Biologists Ltd | Development (2016) 143, 4430-4440 doi:10.1242/dev.141036

RESEARCH ARTICLE

Ligament versus bone cell identity in the zebrafish hyoid skeleton is regulated by *mef2ca*

James T. Nichols[1,*,‡], Bernardo Blanco-Sánchez[1], Elliott P. Brooks[1], Raghuveer Parthasarathy[2], John Dowd[1], Arul Subramanian[3], Gregory Nachtrab[4], Kenneth D. Poss[4], Thomas F. Schilling[3] and Charles B. Kimmel[1]

ABSTRACT

Heightened phenotypic variation among mutant animals is a well-known, but poorly understood phenomenon. One hypothetical mechanism accounting for mutant phenotypic variation is progenitor cells variably choosing between two alternative fates during development. Zebrafish *mef2ca*^{b1086} mutants develop tremendously variable ectopic bone in their hyoid craniofacial skeleton. Here, we report evidence that a key component of this phenotype is variable fate switching from ligament to bone. We discover that a 'track' of tissue prone to become bone cells is a previously undescribed ligament. Fate-switch variability is heritable, and comparing mutant strains selectively bred to high and low penetrance revealed differential *mef2ca* mutant transcript expression between high and low penetrance strains. Consistent with this, experimental manipulation of *mef2ca* mutant transcripts modifies the penetrance of the fate switch. Furthermore, we discovered a transposable element that resides immediately upstream of the *mef2ca* locus and is differentially DNA methylated in the two strains, correlating with differential *mef2ca* expression. We propose that variable transposon epigenetic silencing underlies the variable *mef2ca* mutant bone phenotype, and could be a widespread mechanism of phenotypic variability in animals.

KEY WORDS: Zebrafish, Craniofacial skeleton, *mef2ca*, Bone, Ligament, Variability

INTRODUCTION

When development goes awry in genetic mutants, the resulting phenotypes often vary substantially compared with the wild type (Waddington, 1942). Why some mutants have overt, dramatic phenotypes but their genetically similar mutant siblings appear wild type remains largely mysterious. We previously reported an extremely variable phenotype in the zebrafish *mef2ca*^{b1086} mutant (DeLaurier et al., 2014). *Mef2c* encodes a MADS domain-containing transcription factor crucial for wild-type skeletal development in mice and zebrafish (Arnold et al., 2007; Miller et al., 2007; Verzi et al., 2007). The zebrafish *mef2ca*^{b1086} allele, which contains an early stop codon and is thought to encode just the DNA-binding MADS domain, results in a notably variable ectopic bone phenotype involving the opercle, a bone supporting the gill cover (DeLaurier et al., 2014; Miller et al., 2007). Within this gain-of-bone phenotype, the recurrence of an ectopic bony strut led us to hypothesize that a cryptic developmental pathway present in wild types is revealed in mutants (DeLaurier et al., 2014). Therefore, even in the face of extreme variation, careful study reveals consistencies in the phenotype that can disclose important insights into the developmental mechanisms that underlie the phenotype and its variability.

The larval zebrafish head skeleton consists of a wide array of different cell types including bone-producing osteoblasts and ligament-generating cells ('ligamentoblasts'). Osteoblasts and ligamentoblasts in the head largely originate from a field of neural crest-derived progenitors, which is exposed to signals that regulate the expression of transcription factors (Barske et al., 2016; Medeiros and Crump, 2012). In turn, the transcription factors execute cell fate choices promoting the correct cell type at the proper location. When transcription factor function is disrupted, as in genetic mutants, cells can choose an alternative cell fate such that the animal develops an excess of one cell type at the expense of another. For example, the transcription factor *barx1* controls the choice to become a joint cell versus a cartilage cell in the zebrafish lower jaw, resulting in the gain of joint cells at the expense of cartilage cells in *barx1* mutants (Nichols et al., 2013). *Mef2c* is involved in cell fate decisions in the mouse hematopoietic system (Schüler et al., 2008; Stehling-Sun et al., 2009), motivating the hypothesis that *mef2ca* functions either as a switch or upstream to a switch in the head skeleton. However, what cell types, if any, *mef2ca*^{b1086} mutants lose when they gain osteoblasts has not yet been examined.

Whereas single gene mutations may allow cells to choose an alternative fate, mutant phenotypes are frequently variable and may even include phenotypically wild-type individuals among genotypic mutants, a phenomenon known as incomplete penetrance. It is likely that complex genetics, environmental variations and stochastic developmental noise contribute to the penetrance of mutant phenotypes. One model accounting for variable phenotypes that fall into two classes, affected versus unaffected, is the threshold character model of quantitative genetics (Falconer et al., 1996; Lynch and Walsh, 1998). In the threshold character model, a combination of genes and environment controls a normally unobservable continuous variable termed 'liability', which underlies an outwardly observable phenotype. The threshold model has been invoked to explain the inheritance and incomplete penetrance of human disease alleles (Dipple and McCabe, 2000a,b).

One liability proposed to underlie incomplete penetrance is transcriptional variability (Raj et al., 2010). A recently appreciated source of transcriptional variability that we explore in this study involves mobile repetitive DNA elements, transposons. Transposons can mediate transcriptional variation by interacting

[1]Department of Biology, University of Oregon, Eugene, OR 97403, USA. [2]Department of Physics, University of Oregon, Eugene, OR 97403, USA. [3]Department of Developmental and Cell Biology, University of California, Irvine, Irvine, CA 92697, USA. [4]Department of Cell Biology, Duke University Medical Center, Durham, NC 27710, USA.
*Present address: Department of Craniofacial Biology, School of Dental Medicine, University of Colorado Anschutz Medical Campus, Aurora, CO 80045, USA.

‡Author for correspondence (james.nichols@ucdenver.edu)

J.T.N., 0000-0002-7263-1704

Received 9 June 2016; Accepted 18 October 2016

Development (2016) 143, 4430-4440 doi:10.1242/dev.141036

with host genes in cis to control transcription of nearby genes as well as variably altering the local epigenetic landscape (Feschotte, 2008; Rebollo et al., 2012; Slotkin and Martienssen, 2007; Whitelaw and Martin, 2001). Furthermore, stochastic variation in epigenetic silencing of transposons can account for phenotypic variation, even among genetically identical animals (Morgan et al., 1999; Whitelaw and Martin, 2001). The degree to which transposon-host interactions contribute to wild-type or mutant development remains largely unknown.

Here, we detect consistency among the variable *mef2ca*^{b1086} mutant phenotypes. We find that the earliest manifestation of the ectopic bone phenotype is often the appearance of osteoblasts along a 'track' running perpendicular to the developing opercle. The cells normally in this track are those of a ligament, newly discovered in this study, which appear to be variably 'fate switched' to osteoblasts in the *mef2ca*^{b1086} mutant. Fate-switching variability is heritable such that selective breeding can drive the penetrance of the phenotype up or down, and we have selectively bred two strains to high and low penetrance. We report differential expression of the *mef2ca*^{b1086} mutant allele in our high and low penetrance strains and that overexpression of *mef2ca*^{b1086} mutant transcripts in the low penetrance strain increases fate-switch penetrance whereas knockdown of *mef2ca*^{b1086} translation in the high penetrance strain decreases fate-switch penetrance. Furthermore, differential *mef2ca*^{b1086} expression is correlated with differential DNA methylation on a transposable element at the *mef2ca* locus. From these studies, we propose an epigenetic basis of the phenotypic variation: the expression of the deleterious, likely antimorphic *mef2ca*^{b1086} allele is the liability underlying fate-switch penetrance, which is correlated with variable epigenetic transposon silencing.

RESULTS

A track of cells linking the opercle to the ceratohyal is competent to become osteoblasts in *mef2ca*^{b1086} mutants

The prominent opercle and branchiostegal ray bones in the larval zebrafish head skeleton (Fig. 1A) are variably expanded in *mef2ca*^{b1086} mutants. The phenotype ranges from wild-type-like bones (Fig. 1B, *mef2ca*^{b1086} mild) to large plate-like bony expansions (Fig. 1B, *mef2ca*^{b1086} severe). One recurring mutant phenotype is a skeletal strut or bone bridge orthogonal to the direction of normal opercle growth (Fig. 1B, arrows), leading us to propose that *mef2ca*^{b1086} mutants reveal a cryptic developmental pathway (DeLaurier et al., 2014). Furthermore, we observed that the first ectopic osteoblasts appear along a tissue track orthogonal to the developing opercle. These findings motivated us to assess carefully whether there are any regular patterns of ectopic bone formation in mutants. To this end, time-lapse recordings of *mef2ca*^{b1086} mutant zebrafish carrying the *sp7:EGFP* osteoblast transgene were 'skeletonized' (see Materials and Methods) and aligned to observe more easily the location and direction of the protrusions of ectopic growth (Fig. 1C; Movie 1). In *mef2ca*^{b1086} mutants, the nascent orthotopic opercle grows predominantly in a straight line in the ventral direction, as we have previously described for wild types (Kimmel et al., 2010). However, the skeleton representing the first ectopic osteoblasts in this time-lapse recording reveals their location in a protrusion 40 µm from the dorsal (joint) end of the opercle extending in an essentially straight line orthogonal to the direction of opercle growth (Fig. 1C, arrows). By the final frames, the skeletonized outline reveals the line of orthotopic osteoblasts in the dorsal-ventral axis with the ectopic outgrowth extending along a perpendicular track in the anterior-posterior axis. Thirteen skeletonized *mef2ca*^{b1086} mutant time-lapse recordings were overlaid to uncover any consistencies in the location and orientation of ectopic bone in *mef2ca*^{b1086} mutants (Fig. 1D). Given the extreme variation in late-stage phenotypes (Fig. 1B), we were surprised to discover that both the location and orientation of the earliest ectopic growth is very ordered. The location is consistently between 30 and 70 µm from the dorsal end of the bone along the major axis, and the orientation is almost exclusively orthogonal to the direction of primary opercle growth, thus defining the track of ectopic osteoblasts. These data support our hypothesis that a special population of cells residing in the track perpendicular to the opercle is competent to transform into bone in *mef2ca*^{b1086} mutants.

A clue to the identity of the track of tissue came from observing skeletal mobility in non-anesthetized wild-type larvae during jaw opening (Movie 2). We observed the coordinated movement of the opercle and the adjacent ceratohyal cartilage (Fig. 1E), suggesting that, during the larval stage, some tether links them. Ligaments are cord-like structures that tether bone to bone or bone to cartilage, and we hypothesized that a ligament connects the anterior apex of the opercle to the posterior end of the ceratohyal. To our knowledge, there is no description of such a ligament in any fish.

Molecular markers reveal a newly identified operculohyoid ligament, which is lost when bone is gained in *mef2ca*^{b1086} mutants

To determine whether cells residing in the track between the opercle and ceratohyal have molecular characteristics associated with ligament identity, we developed methods of visualizing ligaments and examined them in wild-type animals. Scleraxis encodes a basic helix-loop-helix transcription factor associated with ligament identity in mouse, chick and zebrafish (Chen and Galloway, 2014; Cserjesi et al., 1995; Schweitzer et al., 2001). Expression of the zebrafish *scleraxis a* co-ortholog (*scxa*) has been reported in the developing pharyngeal skeleton (Chen and Galloway, 2014), although expression at the putative ligament attached to the opercle was not described. We found *scxa* mRNA expression along the track of tissue orthogonal and anterior to the developing opercle described above (Fig. 2A, arrow). A second marker, Thrombospondin 4b (Thbs4b) is an extracellular matrix protein required for tendon attachment in zebrafish (Subramanian and Schilling, 2014, 2015). We detected strong Thbs4b protein immunoreactivity in the track of tissue (Fig. 2B, arrow) extending orthogonal and anterior to the opercle (Fig. 2B, op) matching the observed track of ectopic bone forming cells in Fig. 1D. A third marker of the putative ligament is a member of the aristaless domain-containing family of transcription factors that is expressed in a subset of neural crest-derived craniofacial mesenchyme including early osteoblasts in mice (Hudson et al., 1998; Qu et al., 1997, 1998). In zebrafish, expression of one of these, *alx4a*, marks a subset of the mesenchyme that will develop into craniofacial structures in the head (Dee et al., 2013). Furthermore, *alx4a* regulatory sequences drive transgene expression in osteoblasts and fibroblast-like cells in the anterior pectoral fin (Nachtrab et al., 2013). We found that the *alx4a* transgene is expressed in elongated cells in the track of tissue extending orthogonal to the opercle (Fig. 2C, arrow), as well as more ventrally positioned rounded cells. Imaging the cartilage skeleton along with the *alx4a* reporter revealed that the *alx4a* track terminates at the ceratohyal cartilage as predicted for the ligament in question (Fig. S1), supporting the notion that *alx4a* is expressed in ligament cells. We further note that a subset of osteoblasts in the opercle where the putative ligament attaches to

Development (2016) 143, 4430-4440 doi:10.1242/dev.141036

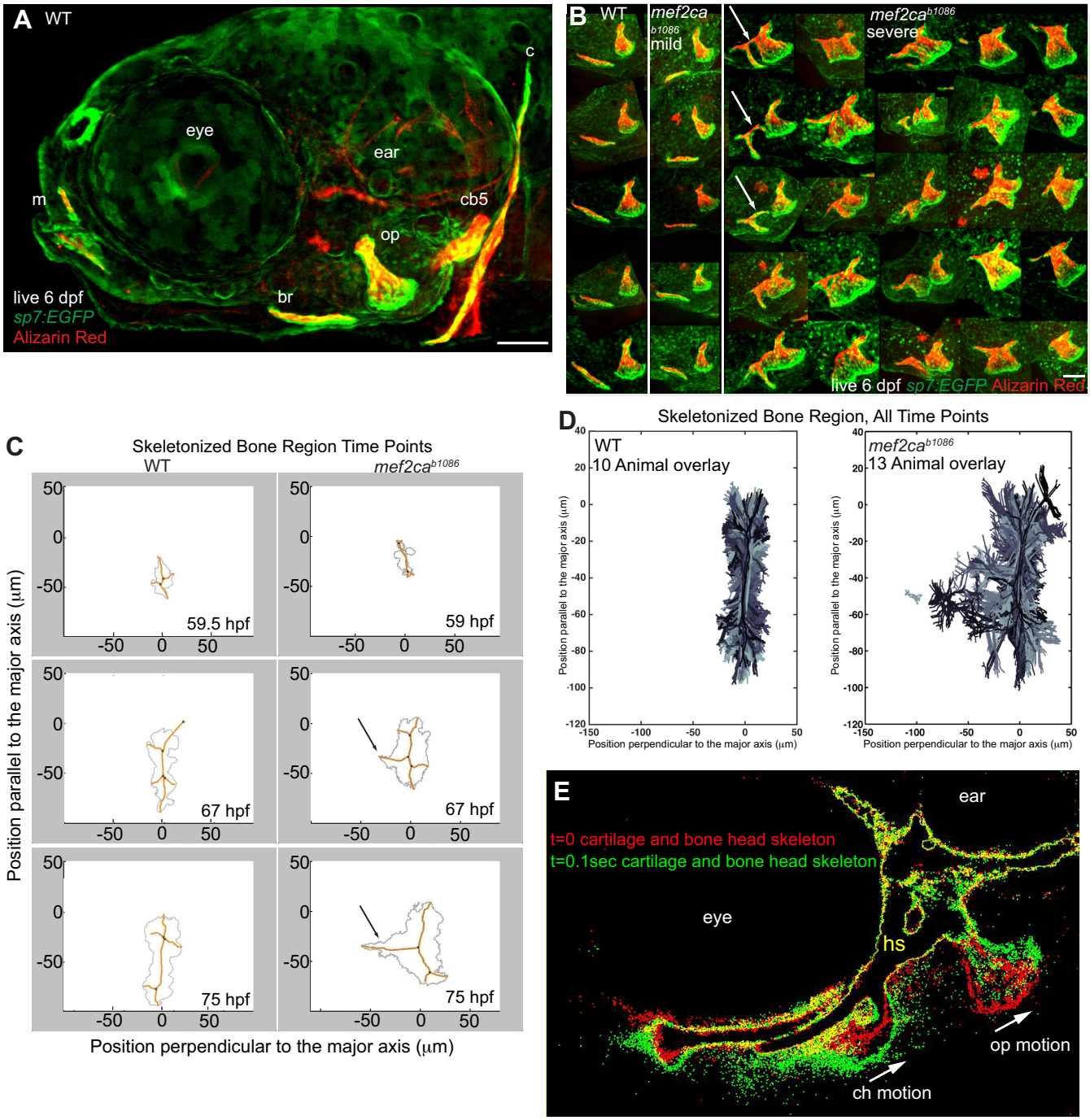

Fig. 1. *mef2ca*^{b1086} bone phenotypes and skeletal motion suggest a unique track of tissue orthogonal to the opercle. (A,B) Confocal projections of osteoblasts (*sp7:EGFP*) and bones (Alizarin Red) from live 6 dpf zebrafish. In A, the opercle (op) branchiostegal ray (br), cleithrum (c) and ceratobranchial 5 (cb5) bony elements are labeled and the eye, ear and mouth (m) are indicated for reference. In B, op and br bone phenotypes in wild types (WT), *mef2ca*^{b1086} mutants with bone phenotypes resembling wild type (*mef2ca*^{b1086} mild), and mutants with bony expansions (*mef2ca*^{b1086} severe) are shown in this composite image. Arrows indicate a narrow track of extra bone. Images are projections of several confocal sections. (C) 'Skeletonized' time-lapse movies tracking the location and direction of ectopic growth (arrows). The major direction of op growth is along the *y*-axis. (D) Overlays of skeletonized time-lapse recordings from wild types and mutants. (E) Excerpts from a movie in which the head skeleton cartilage (*sox9a:EGFP*) and bone (*sp7:EGFP*) were imaged in the same fluorescent channel from a non-anesthetized larva and outlined (red). The same animal was imaged 0.1 s later and the head skeleton was outlined again (green) and overlaid on the first image revealing skeletal motion. All images are lateral views, anterior is towards the left and dorsal is upward in all panels. Scale bars: 100 μm.

this bone also expresses *alx4a* (Fig. 2C, double label). These three labels (*scxa*, Thbs4b and *alx4a*) show that the track of tissue linking the anterior end of the opercle to the posterior end of the ceratohyal in larval zebrafish is a ligament, which we have named the operculohyoid ligament.

In *mef2ca*^{b1086} mutant zebrafish, we found that whenever ectopic osteoblasts were detected by ectopic *sp7* expression, ligament cells were correspondingly lost, revealed by decreased *scxa* expression (Fig. 2D, asterisk), Thrombospondin 4b antibody staining (Fig. 2E, asterisk) or *alx4a* transgene expression (Fig. 2F, asterisk). The

Development (2016) 143, 4430-4440 doi:10.1242/dev.141036

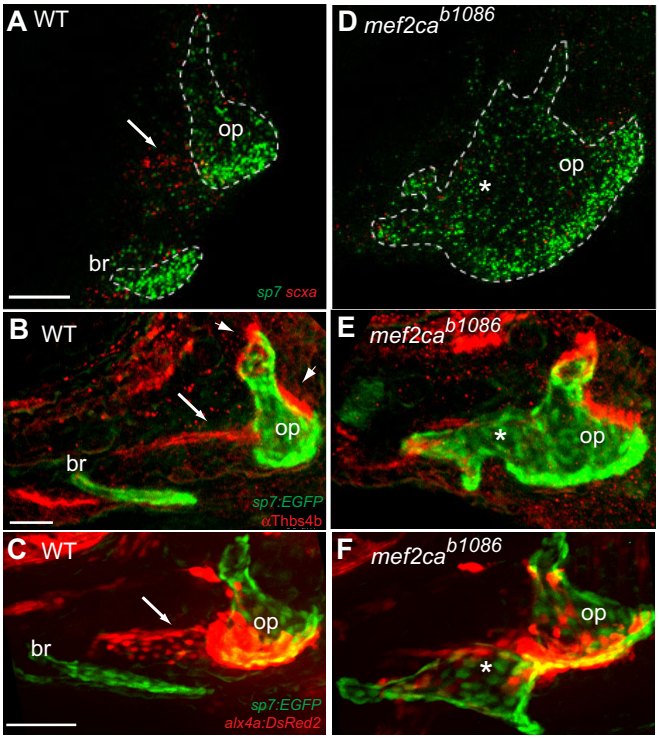

Fig. 2. The orthogonal tissue track has ligament identity, which is lost when ectopic bone develops in *mef2ca*^{b1086}. (A,D) Confocal images of *sp7* (green) and *scxa* (red) transcripts detected by *in situ* hybridization in 5 dpf zebrafish. (B,E) Confocal images of 5 dpf *sp7:EGFP* (green) transgenic larvae immunostained with anti-Thbs4b antibody (red). (C,F) Confocal images of live 6 dpf *sp7:EGFP* (green) and *alx4a*:*DsRed2* (red) transgenic larvae. Wild-type (WT) and mutant (*mef2ca*^{b1086}) images were uniformly adjusted for brightness and contrast. The opercle (op) and branchiostegal ray (br) are indicated. Arrows mark putative ligaments, arrowheads denote tendons, asterisks mark ectopic bone where ligament identity is lost. All images are projections of several confocal sections. Lateral views, anterior is towards the left and dorsal is up. Scale bars: 50 µm.

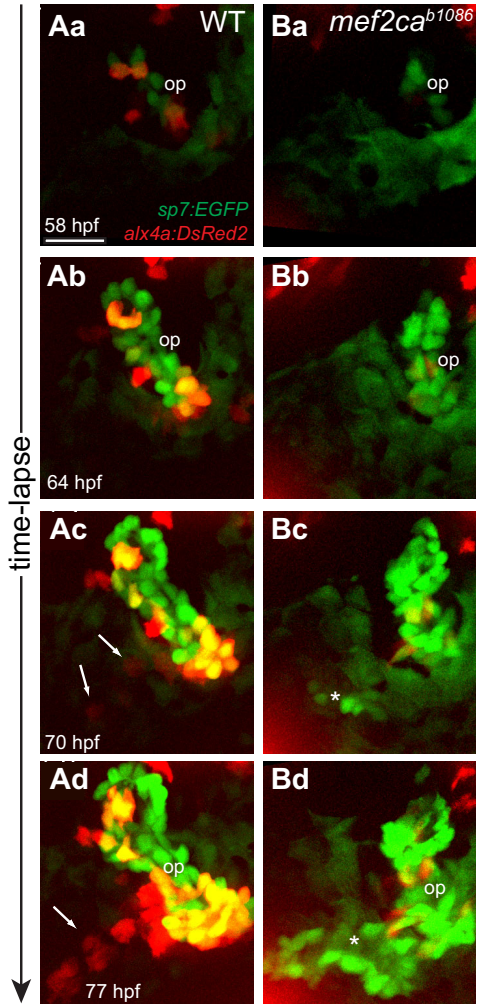

Fig. 3. Ectopic bone cells appear in place of ligament cells in *mef2ca*^{b1086}. (A,B) Excerpts from a time-lapse movie imaging *sp7:EGFP* (green) and *alx4a*:*DsRed2* (red) transgenic larvae. Arrows mark ligament cells, asterisks label ectopic bone cells. Background green fluorescence of the skin is visible in some images. Lateral views, anterior is towards the left and dorsal is up. op, opercle; WT, wild type. Scale bar: 10 µm.

complementary nature of the osteoblast and ligament markers in mutants suggest that bone cells are gained at the expense of ligament cells in *mef2ca*^{b1086} mutants, motivating the hypothesis that cells fated to become ligamentoblasts in wild types can instead fate switch to become osteoblasts in *mef2ca*^{b1086} mutants.

Ligament fate switches to bone in *mef2ca*^{b1086} mutants

To test the fate switch hypothesis, that *mef2ca*^{b1086} mutant progenitor cells adopt the osteoblast cell fate instead of the ligament cell fate, we monitored the differentiation of these two cell types by time-lapse analysis (Movie 3). In these experiments, we found that the first opercle cells initiate *sp7* expression at approximately the same time, 58 h post-fertilization (hpf), and location in wild types and mutants (Fig. 3Aa,Ba, op). We observed that the opercle grows by addition of osteoblasts in the ventral direction in both wild types and mutants (Fig. 3Ab,Bb, op). However, the number of double-positive *sp7;alx4a* cells appeared to be reduced in the mutant, suggesting that the identity of the ligament connection site may already be lost at these early stages. Around 70 hpf, *alx4a* single-positive ligamentoblasts in developing wild-type animals were first detected along the track of tissue orthogonal and anterior to the op (Fig. 3Ac, arrows). Strikingly, in *mef2ca*^{b1086} mutants, ectopic osteoblasts appeared at essentially the same time and place that the ligamentoblasts appeared in wild types (Fig. 3Bc, asterisk). Additional ectopic osteoblasts continued to appear in the mutant concurrent with the decreased appearance of ligament cells (compare Fig. 3Bd, asterisk, with 3Ad, arrow), although additional ectopic bone cells variably develop outside of the ligament track at later stages (Fig. 2D-F; Fig. 3Bd).

The appearance of osteoblasts in mutants at the time and place that ligamentoblasts appear in wild types led us to hypothesize that ectopic bone in mutants originates from progenitor cells that remain in position in the ligament track and differentiate into osteoblasts instead of ligamentoblasts. To test this hypothesis, we generated a transgenic line in which the pharyngeal arch ectomesenchyme progenitor field is labeled with nuclear-localized mCherry (*fli1a:NLSmCherry*) allowing observation of progenitor cells as they differentiate into osteoblasts (Movie 4). Based on these studies, we estimate that the progenitor field is similar in wild types and mutants with respect to size and number of nuclei (Fig. 4Aa,Ba) before any *sp7*-expressing osteoblasts were observed (Fig. 4Ca,Da). A few progenitor cells near the future opercle joint were the first to initiate the osteoblast program as indicated by *sp7* transgene expression (Fig. 4Ab,Bb,Cb,Db, op). Osteoblasts were continuously added to the growing opercle by additional progenitor cells initiating *sp7* expression (Fig. 4Ac,Bc,Cc,Dc). Following well-isolated

Development (2016) 143, 4430-4440 doi:10.1242/dev.141036

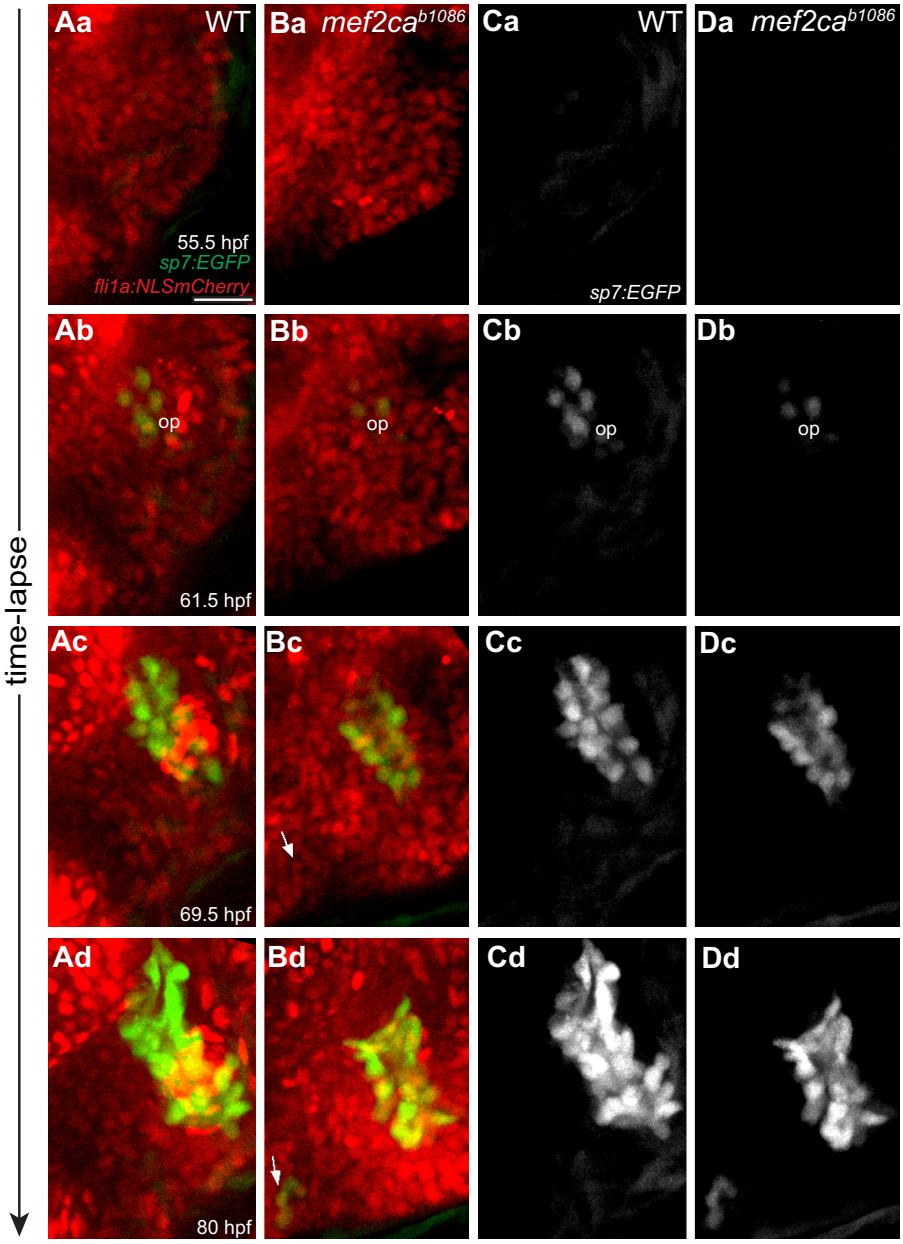

Fig. 4. Progenitor cells remain in position and differentiate into bone in *mef2ca*^{b1086}. (A,B) Excerpts from a time-lapse movie imaging *sp7:EGFP* (green) and *fli1a:NLSmCherry* (red) transgenics. Arrows track a progenitor cell that ectopically initiates *sp7:EGFP* expression. (C,D) *sp7:EGFP* single channel fluorescence from images in A and B. Frames are lateral views, anterior is towards the left and dorsal is up. op, opercle; WT, wild type. Scale bar: 10 µm.

progenitor cell nuclei in mutants (Fig. 4Bc,Bd, arrows) indicated that ectopic osteoblasts originate from the track of cells connecting the opercle and the ceratohyal. Alternatives to the transfating hypothesis are ectopic cell migration, or proliferation of the progenitor field. However, we detect no evidence of these, which would be observable in our time-lapse recordings with *fli1a:NLSmCherry* (Sasaki et al., 2013), ruling out these hypotheses. Another alternative hypothesis regarding the identity of the ectopic bone is that it is a precocious interopercle, a bone that forms anterior to the opercle later in development (Eames et al., 2013). However, when we examined the interopercle in relation to the operculohyoid ligament in wild types we observed that this bone initiates near the interhyal cartilage, far from the opercle, whereas the ectopic bone in *mef2ca*^{b1086} mutants develops adjacent to the opercle. Moreover, we found that the interopercle develops surrounding the operculohyoid ligament (Fig. S2) unlike the ectopic bone in mutants, which is gained at the expense of the operculohyoid ligament. These data are consistent with the conclusion that the ectopic bone in *mef2ca*^{b1086} mutants, in part, originates from fate-switched ligament cells and is not a precocious interopercle.

The penetrance of the ligament-to-bone fate-switching phenotype is heritable

A substantial fraction of the variation observed in *mef2ca*^{b1086} mutants is due to stochastic developmental noise (DeLaurier et al., 2014; see also below). However, we observed that when *mef2ca*^{b1086} mutants develop the mild phenotype (wild-type-like opercles) this phenotype was more often bilateral than expected from chance alone (4/50 observed versus 0.72/50 expected by chance alone; $P<0.0001$, χ^2 analysis). As developmental noise (Polak, 2003) should not often yield such bilateral pairing, we hypothesized that the genetic background also influenced whether the phenotype would be mild or severe. To test this hypothesis we designed a genetic selection experiment based on the classic selective breeding strategy of family selection (progeny testing) (Falconer et al., 1996; Lush, 1935; Lynch and Walsh, 1998;

Development (2016) 143, 4430-4440 doi:10.1242/dev.141036

Prentice, 1935). In our selection experiment, we scored *mef2ca*^{b1086} heterozygous sibling pairs for the penetrance of fate switching in their offspring. Whereas we found that the offspring penetrance was consistent among repeat crosses of the same parental pair (Fig. S3), we discovered a great deal of variation among sibling parental pairs in the first generation, ranging from 2% to 87% penetrance (Fig. 5A, low 1 and high 1). Using this scoring system, we generated two separate selection lines: fish that produced offspring with high penetrance of the ectopic bone phenotype were bred ('upward' selection, which should increase the frequency of the phenotype), whereas in the other line breeding pairs that gave low penetrance were selected ('downward' selection). We found that we could, in a few generations, shift the distribution of offspring penetrance scores both upward and downward as our selection experiment progressed. This experiment clearly demonstrates heritability of fate-switching penetrance. To examine further the nature of heritability, we hybridized pairs of animals from high or low penetrance lines and examined the F1 hybrid generation (Fig. 5B). We found that the F1 progeny had a mean phenotype between that of the parental lines, although the distribution of penetrance in the two F1 families differed slightly and both were skewed towards higher penetrance.

The *mef2ca*^{b1086} mutant transcript is differentially expressed in high and low penetrance strains

What is the selectable difference between high and low penetrance strains? Because the function of the *mef2ca* gene is clearly important for the variable fate choice between ligament versus bone identity, we hypothesized that the expression of *mef2ca* might also be involved in the variable decision to become a ligament or bone cell. To test this hypothesis, we assayed *mef2ca* gene expression in *mef2ca*^{b1086} mutant animals from high and low penetrance strains by *in situ* hybridization. We discovered that *mef2ca*^{b1086} transcript expression appeared to be increased in mutants from the high penetrance strain compared with mutants from the low penetrance strain (Fig. 6A), an observation confirmed by quantitative transcript analyses (Fig. S4).

The severe phenotypes in animals with high quantities of the mutant transcript and mild phenotypes in individuals with low amounts of transcript motivate the hypothesis that strong expression of the *mef2ca*^{b1086} transcript contributes to the severe phenotype in the high penetrance strain. To test this hypothesis directly, we injected *mef2ca*^{b1086} mRNA into mutants from the low penetrance strain (*mef2ca*$^{b1086\text{-}mild}$) and found a significant increase in fate-switching penetrance in injected animals compared with uninjected controls (Fig. 6B, $P<0.01$). Conversely, we knocked down *mef2ca*^{b1086} translation in the high penetrance strain (*mef2ca*$^{b1086\text{-}severe}$) with morpholino injection (Miller et al., 2007) and found a significant decrease in fate-switching penetrance in injected animals compared with uninjected controls (Fig. 6B, $P<0.01$). These findings support the hypothesis that variable expression of *mef2ca*^{b1086} underlies the variable mutant phenotype. Because increased expression of the mutant allele is associated with the more severe phenotype we suggest that the *mef2ca*^{b1086} mutation is antimorphic, as we consider further next.

Fate switching is largely specific to the *mef2ca*^{b1086} allele

That high expression of the *mef2ca*^{b1086} allele promotes fate switching suggests that ligament-to-bone switching is a special feature of this allele. To test directly the hypothesis that high penetrance of fate switching is specific to the *mef2ca*^{b1086} allele, we analyzed another *mef2ca* mutant allele (*mef2ca*^{b631}) in which the initiating methionine is destroyed (Miller et al., 2007). We discovered by pair-wise crossing individual animals from an unselected background that mutants homozygous for the *mef2ca*^{b631} allele had overall very low penetrance of fate switching (Fig. 6C), comparable to our *mef2ca*^{b1086} 'mild' selected line (Fig. 5A, downward selection strain), and that most opercles resembled wild type.

Although both the *mef2ca*^{b631} and *mef2ca*^{b1086} alleles are completely recessive to the wild-type allele, increased expression of the fate-switching *mef2ca*^{b1086} allele increases the penetrance of the phenotype, characteristic of an antimorph. Because antimorphs are characteristically dominant, we wondered if there is ever a genetic context in which the fate-switching *mef2ca*^{b1086} allele can act as a dominant. We tested the hypothesis that *mef2ca*^{b1086} is dominant to *mef2ca*^{b631} by generating heteroallelic combinations. In mutants heteroallelic for *mef2ca*^{b1086} from the mild selected line (*mef2ca*$^{b1086\text{-}mild}$) and *mef2ca*^{b631}, the fate-switching penetrance was low, similar to either the *mef2ca*$^{b1086\text{-}mild}$ or *mef2ca*^{b631} homoallelic mutants. By contrast, in mutants heteroallelic for

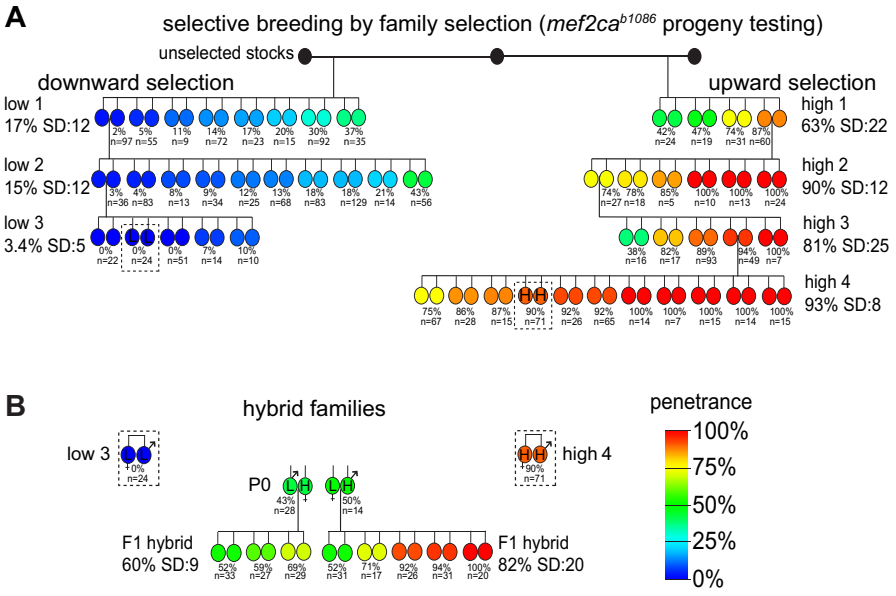

Fig. 5. Selective breeding demonstrates that the *mef2ca*^{b1086} bone phenotype penetrance is heritable. (A) In our selective breeding experiment, we pair-wise crossed siblings heterozygous for the *mef2ca*^{b1086} allele, and homozygous *mef2ca*^{b1086} mutant offspring (lethal) were stained for cartilage and bone at 6 dpf. We scored the proportion of *mef2ca*^{b1086} mutant offspring that develop any ectopic bone on either side, thus calculating the offspring penetrance value that we then assigned to each parental pair. The offspring penetrance values are heat map color coded in this pedigree as indicated. Black circles represent unscored animals. The mean penetrance and standard deviation (SD) at each generation are shown. Heterozygous parents that produced offspring with low penetrance were selectively bred in the downward selection line and heterozygous parents that produced high penetrance offspring were selectively bred in the upward selection line. (B) The low (L) and high (H) penetrance pairs boxed in A were hybridized by reciprocal crosses. F1 hybrid pairs were scored for penetrance as in A.

Development (2016) 143, 4430-4440 doi:10.1242/dev.141036

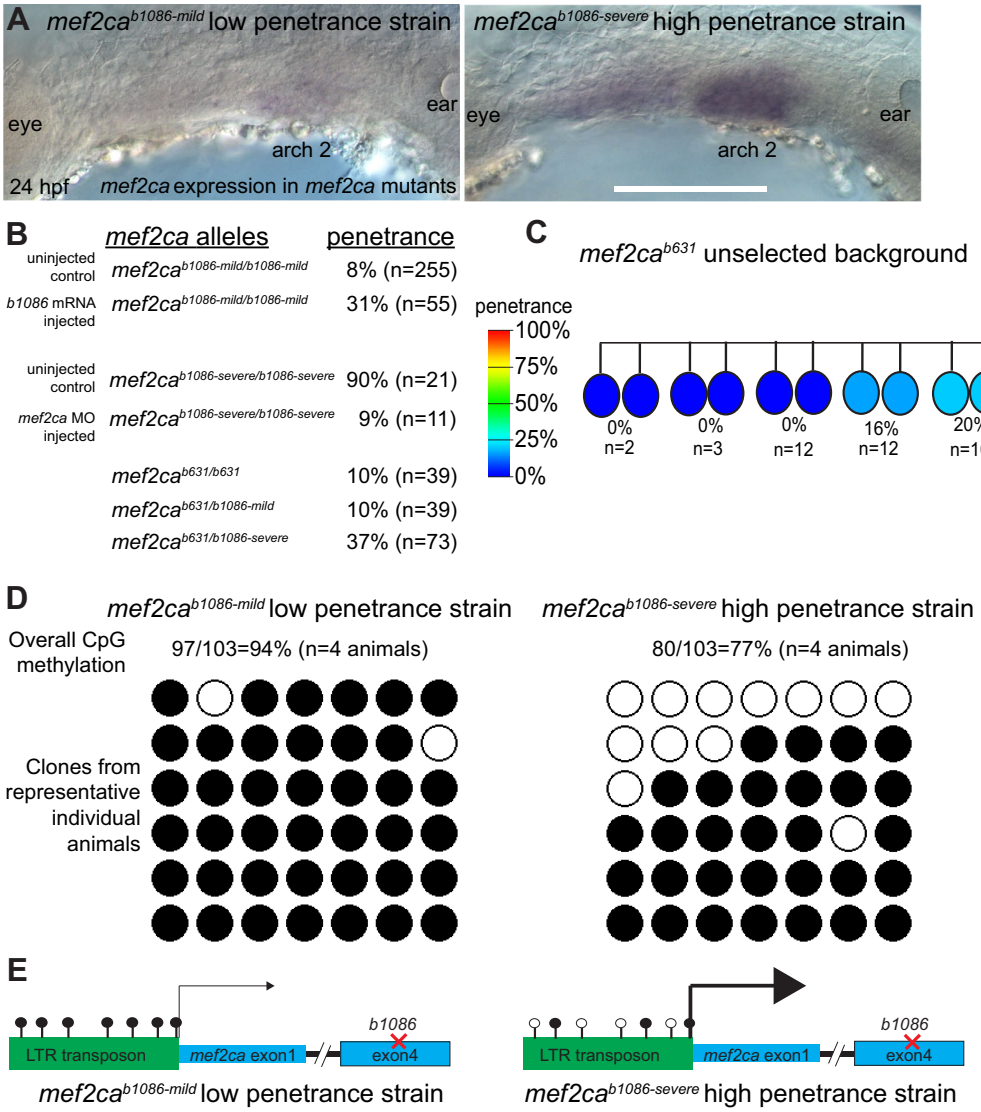

Fig. 6. Differential *mef2ca*^{b1086} transcript expression, transposon DNA methylation and functional consequences. (A) *mef2ca*^{b1086} mutant transcripts were detected by *in situ* hybridization in the low and high penetrance strains. Images are single focal planes, lateral views, anterior is towards the left and dorsal is upward. Scale bar: 100 µm. (B) *mef2ca*^{b1086} mutants from the mild (low penetrance) strain were injected with *mef2ca*^{b1086} mRNA, or *mef2ca*^{b1086} mutants from the severe (high penetrance) strain were injected with *mef2ca* morpholino (MO) and scored for penetrance of ectopic bone. *mef2ca*^{b631} heterozygotes were incrossed, or crossed to *mef2ca*^{b1086} heterozygotes from either the mild or severe strain and *mef2ca* mutant offspring were scored for penetrance of ectopic bone. (E) Full sibling *mef2ca*^{b631} heterozygous adults were crossed in single-pair matings and their *mef2ca*^{b631} homozygous mutant offspring were stained for cartilage and bone and scored at 6 dpf for penetrance of the ligament-to-bone fate-switch phenotype as in Fig. 5. The offspring penetrance score was assigned to the parents, which are color coded as indicated. (D) DNA methylation analysis of 6 dpf *mef2ca*^{b1086} mutant larvae from the low and high penetrance strains. Bisulfite sequencing revealed the overall percentage of CpG methylation of the transposon at the *mef2ca* locus from four animals from each strain. Bisulfite sequencing results from a representative animal from each strain are shown in which six transposon clones from each animal, each with seven CpG sites, were sequenced. Filled circles represent methylated CpG sites. (E) Model for transposon DNA methylation and interaction with the *mef2ca* locus.

mef2ca^{b1086} from the high penetrance strain (*mef2ca*$^{b1086\text{-}severe}$) and *mef2ca*^{b631}, the penetrance was significantly increased relative to *mef2ca*$^{b1086\text{-}mild}$ or *mef2ca*^{b631} homoallelic mutants (Fig. 6B, $P<0.01$). These results resemble those obtained by crossing the *mef2ca*$^{b1086\text{-}severe}$ line to the *mef2ca*$^{b1086\text{-}mild}$ line (Fig. 5B, P0) and suggest that a single copy of the *mef2ca*^{b1086} allele from the severe strain, and any accompanying cis elements, are sufficient to promote fate switching in the mutant context. We interpret these results to indicate that high expression of the *mef2ca*^{b1086} transcript contributes to the severe phenotype beyond a simple loss of function, functioning as an antimorph, as we consider further in the Discussion.

A transposon at the *mef2ca* locus is differentially DNA methylated in high and low penetrance strains

How can we understand heritable, but apparently noisy, variation in transcription of *mef2ca*? Gene expression can be influenced by nearby transposons (Rebollo et al., 2012). Furthermore, variable epigenetic silencing of transposons near endogenous genes mechanistically cause variable phenotypes by impacting local gene expression (Morgan et al., 1999; Rakyan et al., 2003). Therefore, we searched for a transposable element in the zebrafish genome near the *mef2ca* locus that could be mechanistically related to the variable *mef2ca*^{b1086} mutant expression and the resulting phenotypic variation. We identified a candidate Class I long

Development (2016) 143, 4430-4440 doi:10.1242/dev.141036

terminal repeat-containing retrotransposon annotated in the zebrafish genome (Zv9 and GRCz10) at the 5′ end of the *mef2ca* locus, juxtaposed to the annotated *mef2ca* transcriptional start site. Because this transposon, and its epigenetic status, is in a perfect position to impact *mef2ca* expression, we hypothesized that epigenetic silencing at this repetitive element differs between mutants from the high and low penetrance strains. To test this hypothesis, we directly assayed the DNA methylation status of this transposon by sodium bisulfite sequencing in *mef2ca*^{b1086} mutants from the high and low penetrance strains. We found that this transposon was subject to CpG DNA methylation, and discovered that the overall amount of transposon DNA methylation was significantly reduced in the high penetrance strain compared with the low penetrance strain (P<0.01, χ^2 and Fisher's exact test) (Fig. 6D,E). Because the variable methylation status of a transposon juxtaposed to the *mef2ca* locus is associated with high versus low transcription, we propose that a fundamental basis of phenotypic variation in this system is noisy, epigenetic transposon silencing.

DISCUSSION

Variable fate switching in *mef2ca* mutants

Developmental transitions, like cell fate choices, are times of high developmental noise because progenitor cells must destabilize their transcriptional program so that the new program can be adopted. These noisy transition states are probably modulated by the epigenome (Pujadas and Feinberg, 2012). In accordance with this, the fate-switch phenotype in *mef2ca*^{b1086} mutants is especially susceptible to the underlying epigenetic variability. This is a different interpretation from that proposed earlier (DeLaurier et al., 2014), when we speculated that the process of morphogenesis, occurring at a later step in embryonic development, was particularly sensitive to developmental instability. It is intriguing to consider that variable ligament-to-bone fate switching in the hyoid arch might be a deeply conserved phenomenon, as craniofacial ligaments in the hyoid arch of mammals can variably mineralize, exemplified in humans by Eagle's syndrome (Piagkou et al., 2009).

We cannot conclude that *mef2ca* is a general ligament versus bone fate switch, as we do not observe ligaments outside pharyngeal arch 2 fate switching to bone. Rather, our data are consistent with the previously proposed model that *mef2ca* is involved in upstream specification of particular ectomesenchymal lineages, at least in part through its role in dorsal-ventral patterning within the pharyngeal arches, well before the stage when specific differentiated fates develop (DeLaurier et al., 2014; Kimmel et al., 2003; Miller et al., 2007). Here, we report the new discovery that a major aspect of mispatterning in *mef2ca*^{b1086} mutants is a fate switch from ligament to bone. The newly identified ligament in question, which we named the operculohyoid, links the opercle bone to the ceratohyal cartilage, similar to the function performed in most adult teleosts by the interopercular bone as a component of the opercular four-bar lever system (Anker, 1974; Muller, 1996). This ligament has thus far escaped detection in any fish, probably owing to the absence of zebrafish ligament markers, until recently (Chen and Galloway, 2014).

Penetrance is inherited as a threshold character

Rapid phenotype enrichment in our selective breeding experiment suggests that relatively few heritable factors modify the fate switch. The pattern of inheritance we observed appears to fit that of a threshold character in which a continuous, normally unobservable variable controlled by a combination of genes, environment and developmental noise, underlies a phenotype that is easily observed: ligament or bone. In support of the threshold model, we found that family selection (progeny testing) efficiently shifts the proportion of *mef2ca*^{b1086} mutants that display fate switching, a selection method known to be effective for threshold characters (Curnow, 1984). Further support for the threshold model comes from the analysis of our F1 hybrid animals. We find that different parental strains may appear similar in their outward phenotype (high or low penetrance) but the proportion of affected individuals can vary markedly among F1 families, consistent with classical selective breeding experiments testing threshold models (Wright, 1934). Another well-known example of threshold character selection is Waddington's genetic assimilation experiment. He revealed cryptic variation, which he could select upon by inducing environmental stress to move the threshold (Waddington, 1953). In our study, we revealed selectable cryptic variation by disrupting *mef2ca* function. Thus, a quantitative variable probably underlying fate switching in our system is the variation in expression of *mef2ca*^{b1086} due to variable epigenetic silencing of the transposon at the *mef2ca* locus.

Is the inheritance of penetrance genetic or epigenetic?

Our threshold model predicts that we have selected for genetic changes that affect the probability of a particular epigenetic and transcriptional state. That is, the epigenetic variation in our system is modified by genetic variation. However, our experiments cannot rule out a transgenerational epigenetic inheritance model in which we applied selection on the epialleles themselves. The best-documented example of transgenerational epigenetic inheritance is the inheritance of coat color in the agouti viable yellow (A^{vy}) mouse. In A^{vy} mice, a retrotransposon inserted upstream of the agouti locus drives ectopic agouti expression. The transposon is sensitive to silencing by DNA methylation, and the variable DNA methylation pattern results in variable agouti expression and coat color phenotypes that are heritable transgenerationally among isogenic mice (Morgan et al., 1999). The inheritance within an A^{vy} isogenic mouse background demonstrates transgenerational epigenetic (as opposed to genetic) inheritance. Future work recapitulating the *mef2ca*^{b1086} lesion in clonal zebrafish strains (Streisinger et al., 1981) will allow testing for epigenetic inheritance.

mef2ca^{b1086} is a recessive antimorph

Our data are consistent with the model that high expression of the *mef2ca*^{b1086} mutant transcript, when wild-type function is absent, interferes with development beyond a simple loss of function. The *mef2ca*^{b1086} transcript is predicted to encode a C-terminally truncated protein product consisting of essentially just the N-terminal MADS domain that mediates DNA binding and dimerization (Black and Cripps, 2010; Shore and Sharrocks, 1995). Thus, one possible mechanism for the high penetrance ligament-to-bone transformation phenotype is that the high levels of mutant transcript that we showed to be present in the high penetrance strain results in high levels of truncated protein, which has deleterious activity. We find support for this mechanism in our studies of the *mef2ca*^{b631} allele, in which the initiating methionine is destroyed. One potential model is that the *mef2ca*^{b631} allele is a null, because no translated protein is predicted. However, we cannot rule out the possibility that downstream internal translational start sites are functional in *mef2ca*^{b631}. In fact, another methionine is found just 11 amino acids downstream of the *mef2ca*^{b631} mutated methionine, potentially resulting in hypomorphic function. Moreover, the idea that *mef2ca*^{b631} functions as a hypomorph is supported by previous studies with another allele, *mef2ca*^{tn213}, and

Development (2016) 143, 4430-4440 doi:10.1242/dev.141036

mef2ca morpholino injection, which both produce significantly higher penetrance for cartilage phenotypes than *mef2ca*^{b631} (Miller et al., 2007). Nevertheless, the high penetrance of the severe, ligament-to-bone fate-switch phenotype appears to be specific to *mef2ca*^{b1086} probably owing to deleterious activity of this particular allele. We find further support for the model that C-terminally truncated forms of *mef2ca* are detrimental in studies with mammalian cell culture, where expression of C-terminally truncated MEF2 protein fragments interferes with wild-type MEF2C activity (Leupin et al., 2007; Maiti et al., 2008; Molkentin et al., 1996; Ornatsky et al., 1997; Rao et al., 1998). We note that these dominant-negative constructs, encoding both the MADS domain and the adjacent MEF domain, are not precisely identical to *mef2ca*^{b1086}, which is predicted to encode just the MADS domain.

Given this antimorph model for the high penetrance of the *mef2ca*^{b1086} allele, it is not clear why the allele is not inherited as a dominant. Careful examination revealed no phenotypic difference between heterozygotes and homozygous wild types. One possible explanation is that null or hypomorphic alleles can be buffered by a compensatory network (Rossi et al., 2015) or redundant loci, whereas *mef2ca*^{b1086} cannot. In this scenario, *mef2ca*^{b1086} interfering activity is not strong enough to overcome the normal function of wild-type *mef2ca* in the heterozygous condition; it is able only to disrupt the less efficient compensatory or redundant network. Precedent for such an unusual allele comes from work in *Arabidopsis* (Sijacic et al., 2011) in which the authors describe recessive antimorph alleles that can overcome redundant loci but not wild-type alleles. Based on our experimental evidence, we propose that *mef2ca*^{b1086} is a recessive antimorph. With antibodies directed to the N terminus of zebrafish Mef2ca (not currently available) future studies might test directly hypotheses related to the molecular nature of inhibitory activities of the predicted truncated protein.

Epigenetic silencing facilitates canalization

Recent models propose that the epigenome mediates canalization, or the ability of development to produce a consistent phenotype (Pujadas and Feinberg, 2012). Local repetitive elements and their variable silencing influence the expression of genes (Rebollo et al., 2012), and we envisage a general mechanism whereby epigenetic silencing of repetitive elements functions to canalize development by attenuating transcriptional chatter mediated by these transposons. This canalization is especially important in Mendelian mutants to attenuate expression of potentially disruptive mutant alleles such as *mef2ca*^{b1086}. Therefore, Mendelian mutants can be overlaid with complex (epi)genetic traits that contribute to mutant phenotypic variation. Understanding the phenomena that underlie mutant phenotypic variation is not only important for understanding variation in mutant laboratory animals but also human diseases in which Mendelian disorders present with variable penetrance in the clinic (Badano and Katsanis, 2002; Dipple and McCabe, 2000a; Nadeau, 2001).

MATERIALS AND METHODS

Zebrafish lines and husbandry

All fish lines were maintained and staged according to established protocols (Kimmel et al., 1995; Westerfield, 1993). All of our work with zebrafish has been approved by the University of Oregon Institutional Animal Care and Use Committee (IACUC). Assurance number for animal research: A-3009-01. The *mef2ca* mutant alleles *mef2ca*^{b1086} and *mef2ca*^{b631} and their genotyping protocols have been previously described (Miller et al., 2007). KASP genotyping (LGC) and a StepOnePlus Real-Time PCR System (Applied Biosystems) was also used for *mef2ca*^{b1086}. See supplementary Materials and Methods for these and all other primer sequences. The following transgenic lines have been previously described: *Tg(sp7:EGFP)b1212* (DeLaurier et al., 2010), *sox9a:EGFP*^{zc81Tg} (Eames et al., 2013), *Tg(alx4a:DsRed2)pd52* (Nachtrab et al., 2013). To generate *Tg(fli1a:NLSmCherry)b1252*, the *fli1a* ectomesenchyme enhancer (*p5E-fli1a-F-hsp70I*) (Das and Crump, 2012) was recombined upstream of *NLS-mCherry* using the Tol2 kit (Kwan et al., 2007).

Tissue labeling

Alcian Blue and Alizarin Red stains of fixed animals and vital staining with Alizarin Red were performed as described previously (Kimmel et al., 2010; Walker and Kimmel, 2007). Whole-mount Thrombospondin 4b immunostaining was modified from Subramanian and Schilling (2014); details can be found in supplementary Materials and Methods. Whole-mount *in situ* hybridization was carried out as previously described (Talbot et al., 2010) with either fluorescence or immunohistochemical detection. The *sp7* probe has been previously described (DeLaurier et al., 2010). Details describing *mef2ca* and *scxa* probe generation are in supplementary Materials and Methods.

Selective breeding

Full sibling *mef2ca*^{b1086} heterozygous adults were identified by PCR and breeding pairs were isolated and housed separately. Offspring from pairs were stained for cartilage and bone at 6 days post-fertilization (dpf) and *mef2ca*^{b1086} mutant offspring were scored for fate-switch penetrance. Sibling pairs producing offspring with high or low penetrance were selectively bred and phenotypically wild-type animals from these crosses were raised to adulthood for the next generation and next round of selection.

Bisulfite sequencing

DNA was isolated and bisulfite converted with the EZ DNA Methylation Direct Kit (Zymo). Bisulfite-converted transposon DNA was amplified by PCR with primers designed with MethPrimer (Li and Dahiya, 2002). PCR products were cloned using the TOPO TA cloning kit and sequenced with M13R. Analysis of bisulfite data was performed using QUMA (Kumaki et al., 2008). *P*-values were calculated using χ^2 and Fisher's exact tests.

Microscopy and image analysis

Immunohistochemical *in situ*-stained animals were imaged on a Zeiss Axiophot 2. Static confocal images were captured using either a Zeiss LSM5 Pascal confocal or a Leica SD6000 spinning disk confocal. Images were assembled in ImageJ, metamorph and Photoshop with any adjustments applied to all panels. For time-lapse movies, animals were imaged as reported (Huycke et al., 2012) and skeletonized as described in supplementary Materials and Methods and Fig. S5.

mef2ca overexpression, morpholino knockdown and quantification

RNA was extracted from a pool of whole 24 hpf embryos from the high penetrance strain using TRIzol (Thermo Fisher Scientific). cDNA was retrotranscribed using the SuperScript III Kit (Thermo Fisher Scientific). Using the *mef2ca* BC070007.1 sequence as a reference, we amplified cDNA containing the T7 promoter followed by the *mef2ca* native Kozak sequence, the *mef2ca* open reading frame and partial 3′UTR. Amplified fragments were cloned using pCR-Blunt II-TOPO, and *mef2ca*^{b1086} clones were identified by Sanger sequencing. Using Phusion polymerase (NEB), a *mef2ca*^{b1086} cDNA template was amplified from the cloned plasmid and RNA for injection was synthesized using the T7 mMessage Machine transcription kit (Thermo Fisher Scientific). RNA was purified by lithium chloride precipitation. A final RNA dose of 300 pg was injected into one-cell-stage embryos from the *mef2ca*$^{b1086\text{-}mild}$ low penetrance strain. A final dose of 2-3 ng *mef2ca* mRNA translation-blocking morpholino (Miller et al., 2007) was injected into one- to four-cell-stage embryos from the *mef2ca*$^{b1086\text{-}severe}$ high penetrance strain. Injection volumes were estimated using a stage micrometer. *mef2ca* transcripts were quantified by reverse transcription qPCR; see supplementary Materials and Methods for details.

Acknowledgements
We thank Thomas Desvignes for help with qPCR, Aniket Gore for help with bisulfite sequencing, and Mckenna Fairey for help scoring skeletal phenotypes. We are grateful for discussions with our colleagues especially John Postlethwait, Bill Cresko, Monte Westerfield, Anne Ferguson-Smith and Mike Miller.

Competing interests
The authors declare no competing or financial interests.

Author contributions
J.T.N. and C.B.K. conceived and designed experiments. J.T.N., B.B.-S., E.P.B., R.P., J.D., A.S., G.N. and K.D.P. contributed to the acquisition of the data. J.T.N., B.B.-S., E.P.B., R.P., J.D., A.S., T.F.S. and C.B.K. analyzed the data. J.T.N. wrote the paper.

Funding
This research was supported by the National Institutes of Health (NIH) [K99/R00 DE024190 to J.T.N., R01 GM074057 to K.D.P., R21 AR62792 and R01 HD73182 to T.F.S., RO1 DE13834 and PO1 HD22486 to C.B.K.]. Deposited in PMC for release after 12 months.

Supplementary information
Supplementary information available online at
http://dev.biologists.org/lookup/doi/10.1242/dev.141036.supplemental

References

Anker, G. (1974). Morphology and kinetics of the head of the stickleback, Gasterosteus aculeatus. *Trans. Zool. Soc. Lond.* **32**, 311-416.
Arnold, M. A., Kim, Y., Czubryt, M. P., Phan, D., McAnally, J., Qi, X., Shelton, J. M., Richardson, J. A., Bassel-Duby, R. and Olson, E. N. (2007). MEF2C transcription factor controls chondrocyte hypertrophy and bone development. *Dev. Cell* **12**, 377-389.
Badano, J. L. and Katsanis, N. (2002). Beyond Mendel: an evolving view of human genetic disease transmission. *Nat. Rev. Genet.* **3**, 779-789.
Barske, L., Askary, A., Zuniga, E., Balczerski, B., Bump, P., Nichols, J. T. and Crump, J. G. (2016). Competition between jagged-notch and endothelin1 signaling selectively restricts cartilage formation in the zebrafish upper face. *PLoS Genet.* **12**, e1005967.
Black, B. L. and Cripps, R. M. (2010). Myocyte enhancer factor 2 transcription factors in heart development and disease. In *Heart Development and Regeneration*, Vol. 2, 1st edn (ed. N. Rosenthal and R. Harvey), pp. 673-699. Oxford, UK: Academic Press.
Chen, J. W. and Galloway, J. L. (2014). The development of zebrafish tendon and ligament progenitors. *Development* **141**, 2035-2045.
Cserjesi, P., Brown, D., Ligon, K. L., Lyons, G. E., Copeland, N. G., Gilbert, D. J., Jenkins, N. A. and Olson, E. N. (1995). Scleraxis: a basic helix-loop-helix protein that prefigures skeletal formation during mouse embryogenesis. *Development* **121**, 1099-1110.
Curnow, R. N. (1984). Progeny testing for all-or-none traits when a multifactorial model applies. *Biometrics* **40**, 375-382.
Das, A. and Crump, J. G. (2012). Bmps and Id2a Act upstream of Twist1 to restrict ectomesenchyme potential of the cranial neural crest. *PLoS Genet.* **8**, e1002710.
Dee, C. T., Szymoniuk, C. R., Mills, P. E. D. and Takahashi, T. (2013). Defective neural crest migration revealed by a zebrafish model of Alx1-related frontonasal dysplasia. *Hum. Mol. Genet.* **22**, 239-251.
DeLaurier, A., Eames, B. F., Blanco-Sánchez, B., Peng, G., He, X., Swartz, M. E., Ullmann, B., Westerfield, M. and Kimmel, C. B. (2010). Zebrafish *sp7:EGFP*: a transgenic for studying otic vesicle formation, skeletogenesis, and bone regeneration. *Genesis* **48**, 505-511.
DeLaurier, A., Huycke, T. R., Nichols, J. T., Swartz, M. E., Larsen, A., Walker, C., Dowd, J., Pan, L., Moens, C. B. and Kimmel, C. B. (2014). Role of *mef2ca* in developmental buffering of the zebrafish larval hyoid dermal skeleton. *Dev. Biol.* **385**, 189-199.
Dipple, K. M. and McCabe, E. R. B. (2000a). Modifier genes convert 'simple' Mendelian disorders to complex traits. *Mol. Genet. Metab.* **71**, 43-50.
Dipple, K. M. and McCabe, E. R. B. (2000b). Phenotypes of patients with 'simple' Mendelian disorders are complex traits: thresholds, modifiers, and systems dynamics. *Am. J. Hum. Genet.* **66**, 1729-1735.
Eames, B. F., DeLaurier, A., Ullmann, B., Huycke, T. R., Nichols, J. T., Dowd, J., McFadden, M., Sasaki, M. M. and Kimmel, C. B. (2013). FishFace: interactive atlas of zebrafish craniofacial development at cellular resolution. *BMC Dev. Biol.* **13**, 23.
Falconer, D. S. and Mackay, T. F. (1996). *Introduction to Quantitative Genetics*, 4th edn. Cambridge, UK: Pearson.
Feschotte, C. (2008). Transposable elements and the evolution of regulatory networks. *Nat. Rev. Genet.* **9**, 397-405.
Hudson, R., Taniguchi-Sidle, A., Boras, K., Wiggan, O. N. and Hamel, P. A. (1998). Alx-4, a transcriptional activator whose expression is restricted to sites of epithelial-mesenchymal interactions. *Dev. Dyn.* **213**, 159-169.
Huycke, T. R., Eames, B. F. and Kimmel, C. B. (2012). Hedgehog-dependent proliferation drives modular growth during morphogenesis of a dermal bone. *Development* **139**, 2371-2380.
Kimmel, C. B., Ballard, W. W., Kimmel, S. R., Ullmann, B. and Schilling, T. F. (1995). Stages of embryonic development of the zebrafish. *Dev. Dyn.* **203**, 253-310.
Kimmel, C. B., Ullmann, B., Walker, M., Miller, C. T. and Crump, J. G. (2003). Endothelin 1-mediated regulation of pharyngeal bone development in zebrafish. *Development* **130**, 1339-1351.
Kimmel, C. B., DeLaurier, A., Ullmann, B., Dowd, J. and McFadden, M. (2010). Modes of developmental outgrowth and shaping of a craniofacial bone in zebrafish. *PLoS ONE* **5**, e9475.
Kumaki, Y., Oda, M. and Okano, M. (2008). QUMA: quantification tool for methylation analysis. *Nucleic Acids Res.* **36**, W170-W175.
Kwan, K. M., Fujimoto, E., Grabher, C., Mangum, B. D., Hardy, M. E., Campbell, D. S., Parant, J. M., Yost, H. J., Kanki, J. P. and Chien, C.-B. (2007). The Tol2kit: a multisite gateway-based construction kit for Tol2 transposon transgenesis constructs. *Dev. Dyn.* **236**, 3088-3099.
Leupin, O., Kramer, I., Collette, N. M., Loots, G. G., Natt, F., Kneissel, M. and Keller, H. (2007). Control of the SOST bone enhancer by PTH using MEF2 transcription factors. *J. Bone Miner. Res.* **22**, 1957-1967.
Li, L.-C. and Dahiya, R. (2002). MethPrimer: designing primers for methylation PCRs. *Bioinformatics* **18**, 1427-1431.
Lush, J. L. (1935). Progeny test and individual performance as indicators of an animal's breeding value. *J. Dairy Sci.* **18**, 1-19.
Lynch, M. and Walsh, B. (1998). *Genetics and Analysis of Quantitative Traits*. Sunderland, MA: Sinauer.
Maiti, D., Xu, Z. and Duh, E. J. (2008). Vascular endothelial growth factor induces MEF2C and MEF2-dependent activity in endothelial cells. *Invest. Ophthalmol. Vis. Sci.* **49**, 3640-3648.
Medeiros, D. M. and Crump, J. G. (2012). New perspectives on pharyngeal dorsoventral patterning in development and evolution of the vertebrate jaw. *Dev. Biol.* **371**, 121-135.
Miller, C. T., Swartz, M. E., Khuu, P. A., Walker, M. B., Eberhart, J. K. and Kimmel, C. B. (2007). *mef2ca* is required in cranial neural crest to effect Endothelin1 signaling in zebrafish. *Dev. Biol.* **308**, 144-157.
Molkentin, J. D., Black, B. L., Martin, J. F. and Olson, E. N. (1996). Mutational analysis of the DNA binding, dimerization, and transcriptional activation domains of MEF2C. *Mol. Cell. Biol.* **16**, 2627-2636.
Morgan, H. D., Sutherland, H. G., Martin, D. I. and Whitelaw, E. (1999). Epigenetic inheritance at the agouti locus in the mouse. *Nat. Genet.* **23**, 314-318.
Muller, M. (1996). A novel classification of planar four-bar linkages and its application to the mechanical analysis of animal systems. *Philos. Trans. R. Soc. B Biol. Sci.* **351**, 689-720.
Nachtrab, G., Kikuchi, K., Tornini, V. A. and Poss, K. D. (2013). Transcriptional components of anteroposterior positional information during zebrafish fin regeneration. *Development* **140**, 3754-3764.
Nadeau, J. H. (2001). Modifier genes in mice and humans. *Nat. Rev. Genet.* **2**, 165-174.
Nichols, J. T., Pan, L., Moens, C. B. and Kimmel, C. B. (2013). *barx1* represses joints and promotes cartilage in the craniofacial skeleton. *Development* **140**, 2765-2775.
Ornatsky, O. I., Andreucci, J. J. and McDermott, J. C. (1997). A dominant-negative form of transcription factor MEF2 inhibits myogenesis. *J. Biol. Chem.* **272**, 33271-33278.
Piagkou, M., Anagnostopoulou, S., Kouladouros, K. and Piagkos, G. (2009). Eagle's syndrome: a review of the literature. *Clin. Anat.* **22**, 545-558.
Polak, M. (2003). *Developmental Instability: Causes and Consequences*. New York: Oxford University Press.
Prentice, E. P. (1935). *Breeding Profitable Dairy Cattle: A New Source of National Wealth*. Boston, New York: Houghton Mifflin.
Pujadas, E. and Feinberg, A. P. (2012). Regulated noise in the epigenetic landscape of development and disease. *Cell* **148**, 1123-1131.
Qu, S., Li, L. and Wisdom, R. (1997). Alx-4: cDNA cloning and characterization of a novel paired-type homeodomain protein. *Gene* **203**, 217-223.
Qu, S., Tucker, S. C., Ehrlich, J. S., Levorse, J. M., Flaherty, L. A., Wisdom, R. and Vogt, T. F. (1998). Mutations in mouse Aristaless-like4 cause Strong's luxoid polydactyly. *Development* **125**, 2711-2721.
Raj, A., Rifkin, S. A., Andersen, E. and van Oudenaarden, A. (2010). Variability in gene expression underlies incomplete penetrance. *Nature* **463**, 913-918.
Rakyan, V. K., Chong, S., Champ, M. E., Cuthbert, P. C., Morgan, H. D., Luu, K. V. K. and Whitelaw, E. (2003). Transgenerational inheritance of epigenetic states at the murine AxinFu allele occurs after maternal and paternal transmission. *Proc. Natl. Acad. Sci. USA* **100**, 2538-2543.
Rao, S., Karray, S., Gackstetter, E. R. and Koshland, M. E. (1998). Myocyte enhancer factor-related B-MEF2 is developmentally expressed in B cells and regulates the immunoglobulin J chain promoter. *J. Biol. Chem.* **273**, 26123-26129.

Development (2016) 143, 4430-4440 doi:10.1242/dev.141036

Rebollo, R., Romanish, M. T. and Mager, D. L. (2012). Transposable elements: an abundant and natural source of regulatory sequences for host genes. *Annu. Rev. Genet.* **46**, 21-42.

Rossi, A., Kontarakis, Z., Gerri, C., Nolte, H., Hölper, S., Krüger, M. and Stainier, D. Y. (2015). Genetic compensation induced by deleterious mutations but not gene knockdowns. *Nature* **524**, 230-233.

Sasaki, M. M., Nichols, J. T. and Kimmel, C. B. (2013). *edn1* and *hand2* interact in early regulation of pharyngeal arch outgrowth during zebrafish development. *PLoS ONE* **8**, e67522.

Schüler, A., Schwieger, M., Engelmann, A., Weber, K., Horn, S., Müller, U., Arnold, M. A., Olson, E. N. and Stocking, C. (2008). The MADS transcription factor Mef2c is a pivotal modulator of myeloid cell fate. *Blood* **111**, 4532-4541.

Schweitzer, R., Chyung, J. H., Murtaugh, L. C., Brent, A. E., Rosen, V., Olson, E. N., Lassar, A. and Tabin, C. J. (2001). Analysis of the tendon cell fate using Scleraxis, a specific marker for tendons and ligaments. *Development* **128**, 3855-3866.

Shore, P. and Sharrocks, A. D. (1995). The MADS-box family of transcription factors. *Eur. J. Biochem.* **229**, 1-13.

Sijacic, P., Wang, W. Liu, Z. (2011). Recessive antimorphic alleles overcome functionally redundant loci to reveal TSO1 function in Arabidopsis flowers and meristems. *PLOS Genet*. **7**, e1002352.

Slotkin, R. K. and Martienssen, R. (2007). Transposable elements and the epigenetic regulation of the genome. *Nat. Rev. Genet.* **8**, 272-285.

Stehling-Sun, S., Dade, J., Nutt, S. L., DeKoter, R. P. and Camargo, F. D. (2009). Regulation of lymphoid versus myeloid fate 'choice' by the transcription factor Mef2c. *Nat. Immunol.* **10**, 289-296.

Streisinger, G., Walker, C., Dower, N., Knauber, D. and Singer, F. (1981). Production of clones of homozygous diploid zebra fish (Brachydanio rerio). *Nature* **291**, 293-296.

Subramanian, A. and Schilling, T. F. (2014). Thrombospondin-4 controls matrix assembly during development and repair of myotendinous junctions. *eLife* **3**, e02372.

Subramanian, A. and Schilling, T. F. (2015). Tendon development and musculoskeletal assembly: emerging roles for the extracellular matrix. *Development* **142**, 4191-4204.

Talbot, J. C., Johnson, S. L. and Kimmel, C. B. (2010). *hand2* and Dlx genes specify dorsal, intermediate and ventral domains within zebrafish pharyngeal arches. *Development* **137**, 2507-2517.

Verzi, M. P., Agarwal, P., Brown, C., McCulley, D. J., Schwarz, J. J. and Black, B. L. (2007). The transcription factor MEF2C is required for craniofacial development. *Dev. Cell* **12**, 645-652.

Waddington, C. H. (1942). Canalization of development and the inheritance of acquired characters. *Nature* **150**, 563-565.

Waddington, C. H. (1953). Genetic assimilation of an acquired character. *Evolution* **7**, 118-126.

Walker, M. B. and Kimmel, C. B. (2007). A two-color acid-free cartilage and bone stain for zebrafish larvae. *Biotech. Histochem.* **82**, 23-28.

Westerfield, M. (1993). *The Zebrafish Book: A Guide for the Laboratory Use of Zebrafish (*Brachydanio rerio*)*, 3rd edn. Eugene, OR: University of Oregon Press.

Whitelaw, E. and Martin, D. I. K. (2001). Retrotransposons as epigenetic mediators of phenotypic variation in mammals. *Nat. Genet.* **27**, 361-365.

Wright, S. (1934). The results of crosses between inbred strains of guinea pigs, differing in number of digits. *Genetics* **19**, 537.